


 Cite this: *RSC Adv.*, 2022, 12, 6738

# Influence of gardenia yellow on *in vitro* slow starch digestion and its action mechanism†

 Shuncheng Ren,<sup>ID</sup>\* Yi Wan, Xiaoi Zhu,<sup>ID</sup>\* Zelong Liu, Wenhong Zhao, Dongdong Xie and Shenli Wang

This study aimed to explore the influence of gardenia yellow on *in vitro* wheat starch digestion. The influence of gardenia yellow on the digestion properties of starch was determined through *in vitro* digestion, and its action mechanism on slow starch digestion was revealed by laser scanning confocal microscopy, enzymatic inhibition dynamics, and other means of characterization. Results showed that gardenia yellow could inhibit starch digestion, significantly increase the resistant starch and slowly digestible starch contents in starch ( $P < 0.05$ ), and trigger the decrease in glycemic and hydrolysis indices. Furthermore, gardenia yellow could spontaneously bind to the catalytic sites of  $\alpha$ -amylase and  $\alpha$ -glucosidase, affect their secondary structures through vdW force and hydrophobic interaction, and reduce their catalytic abilities to inhibit the digestion process of wheat starch. Therefore, the interactions of gardenia yellow with starch and digestive enzymes jointly promote the slow digestion of starch.

 Received 11th November 2021  
 Accepted 16th February 2022

DOI: 10.1039/d1ra08276k

[rsc.li/rsc-advances](https://rsc.li/rsc-advances)

## 1. Introduction

As a metabolic disease resulting from the comprehensive action of multiple pathogeneses, diabetes is characterized by chronic hyperglycemia and metabolic disorders of sugar, fat, and protein due to insulin hyposecretion. The World Health Organization (WHO) classifies diabetes into two major types: types I and II diabetes; the former is featured by low plasma insulin level because of the destruction of pancreatic  $\beta$ -cells, and the latter is a noninfectious chronic metabolic syndrome manifested by hyperglycemia arising out of impaired insulin secretion and target tissue resistance against insulin action.<sup>1</sup> Type II diabetes is the most common type of diabetes all over the world, accounting for over 90%, and it has been accepted as the main public health problem.<sup>2</sup> By 2030, diabetes, recognized as a “silent killer,” is predicted to become the seventh largest lethal factor of human beings, and the number of people affected by it will increase to 592 million.<sup>3</sup> The latest statistical data released by the WHO showed that approximately 1.5 billion adults worldwide are overweight and obese, and they are susceptible to the potential risk of diabetes.<sup>4</sup> Although diabetes may be triggered by various factors, the dietary pattern plays a sign remarkable role in the prevention of diabetes, and it has aroused extensive attention.

Starch, a major component in human diets, is inseparable from human metabolism, and it has an especially greater

bearing on patients with diabetes.<sup>5</sup> Controlling the glucose level has always been an effective method of relieving diabetes and preventing diabetic complications. During the digestion process of food, starch is hydrolyzed into monosaccharides by  $\alpha$ -amylase and  $\alpha$ -glucosidase in the digestive tract, and the elevation of postprandial blood glucose could be significantly reduced by inhibiting these hydrolases.<sup>6</sup> An effective path to prevent type II diabetes is to repress the starch hydrolysis and glucose absorption. Therefore, researching and developing new-type amylase inhibitors are important. The most effective oral hypoglycemic drug in the market at present is acarbose, which has been widely clinically used as a drug inhibiting the activity of glycosidase, delaying the glucose absorption, and repressing postprandial hyperglycemia. Although it could effectively prevent the elevation of postprandial blood glucose level, acarbose intake could lead to adverse reactions, such as diarrhea, stomachache, abdominal distention, and hepatopathy.<sup>7</sup> Therefore, a promising method may be seeking for safe and effective active substances, which could inhibit starch digestion, from natural plant extracts to prevent and treat diabetes.

The treatment of diabetes with plant extracts has been widely reported.<sup>8</sup> Approximately over 800 plant extracts may exert positive effects on relieving diabetic symptoms.<sup>9</sup> *Gardenia jasminoides* Ellis, being a food and medicine rich in functional components, belongs to the traditional Chinese herbal medicine used to treatment diabetes, with various pharmacological actions, such as antiinflammation, antioxidation, and neuroprotection.<sup>10–13</sup> The extract gardenia yellow from *Gardenia jasminoides* Ellis is also a water-soluble carotene-type natural pigment rarely seen in nature. It has been widely applied to various fields, such as food, as a natural pigment, especially

School of Food Science and Technology, Henan University of Technology, Zhengzhou 450001, P. R. China. E-mail: [scrcn@163.com](mailto:scrcn@163.com); [zhuxiaoi@haut.edu.cn](mailto:zhuxiaoi@haut.edu.cn); Fax: +86-371-67789817; +86-371-67758018; Tel: +86-371-68883238; +86-371-67758018

† Electronic supplementary information (ESI) available. See DOI: 10.1039/d1ra08276k



having excellent coloring effects on macromolecules, including starch and protein. Although gardenia yellow has been extensively applied as a natural coloring agent, its influence on starch digestion has been scarcely reported. Therefore, in this study, the influence of gardenia yellow on the *in vitro* digestion characteristics of wheat starch was explored, and its blood glucose control mechanism was further expounded, with an expectation to lay a theoretical foundation for the development of functional foods for diabetics.

## 2. Materials and methods

### 2.1. Materials

Gardenia yellow (crocin HPLC >90%, crocetin HPLC >9%) was obtained from Henan Zhongda Hengyuan Biotechnology Co., Ltd (Luohe, Henan Province, China), the chemical structures of crocin and crocetin in ESI Fig. S1.† Wheat starch (water content: 12.89%) was bought from Taizhou Haoshihui Seasoning Co., Ltd (Taizhou, Jiangsu Province, China).

### 2.2. Chemical reagents

*p*-Nitrophenyl- $\alpha$ -D-glucopyranoside (*p*NPG) was obtained from Beijing Suolaibao Technological Co., Ltd (Beijing, China). Pig pancreatic  $\alpha$ -amylase was bought from Sigma Chemical Co. (St. Louis, MO, USA), and yeast  $\alpha$ -glucosidase was obtained from Shanghai Yuanye Biotech Co., Ltd (Shanghai, China). The remaining reagents were all purchased from Zhengzhou Xinfeng Assay Device Co., Ltd (Zhengzhou, Henan Province, China).

### 2.3. *In vitro* starch digestion

Slight modifications were made using Englyst method as reference<sup>14</sup>: 0.2 g of starch samples with gardenia yellow contents of 0%, 0.1%, 0.5%, 1%, and 2% was taken, and each sample was placed into a 25 mL test tube. Then, 5 mL of sodium acetate buffer solution (0.2 M, pH 5.2) was added, and after full oscillation and blending, the mixture was gelatinized in a thermostat water bath kettle (80 °C) for 30 min. Next, the mixture was cooled and balanced at 37 °C for 15 min. Five mL of digestive enzyme mixed with liquor containing  $\alpha$ -amylase (300 U mL<sup>-1</sup>) and  $\alpha$ -glucosidase (60 U mL<sup>-1</sup>) was then taken and placed into each test tube, in which two glass beads were added. The mixture was fully oscillated and blended, accurate time-keeping was performed, and 1 mL of hydrolysate was taken out of each test tube and placed in a centrifugal tube at 0, 20, 60, 120, and 180 min. Subsequently, enzyme deactivation was carried out using 5 mL of absolute ethyl alcohol, followed by centrifugation at a rate of 3000 rpm for 10 min. Then, 1 mL of supernatant was taken out of the centrifugal tube, and the concentration of glucose released was measured using 3,5-dinitrosalicylic acid (DNS) method. Parallel determination was conducted three times for each group of samples, and the calculation formulas are as below:<sup>15</sup>

Rapid digestive starch:

$$\text{RDS (\%)} = (G_{20} - \text{FG}) \times 0.9/\text{TS} \times 100, \quad (1)$$

Slow digestive starch:

$$\text{SDS (\%)} = (G_{120} - G_{20}) \times 0.9/\text{TS} \times 100, \quad (2)$$

Resistant starch:

$$\text{RS (\%)} = (1 - [\text{RDS} + \text{SDS}]) \times 100, \quad (3)$$

$$\text{AUC} = C_{\infty}(t_f - t_0) - (C_{\infty}/k)\{1 - \exp[-\Phi(t_f - t_0)]\}, \quad (4)$$

$$\text{HI} = \text{AUC}_G/\text{AUC}_W, \quad (5)$$

$$\text{GI} = 39.71 + 0.549 \text{ HI}, \quad (6)$$

$$\% \text{SH} = 0.9 \times \text{GP}/\text{TS}, \quad (7)$$

where  $G_0$  is the glucose content contained in starch before enzymolysis, mg;  $G_{20}$  is the glucose content contained in starch at 20 min after hydrolysis, mg;  $G_{120}$  is the glucose content contained in starch at 120 min after hydrolysis, mg; TS denotes the total starch content in the sample, mg;  $C_{\infty}$  is the equilibrium concentration of hydrolyzed starch within infinite time;  $t_f$  is the final digestion time (180 min);  $t_0$  represents the initial time (0 min);  $\Phi$  is a kinetic constant; AUC means the area under the curve of reaction;  $\text{AUC}_G$  is the area under the curve of starch reaction in the sample group;  $\text{AUC}_W$  is the area under the curve of reaction in the blank group; HI is the starch hydrolysis index; GI is the glycemic index; %SH is the total amount of starch hydrolyzed; and GP is the glucose production, mg.

The starch digestion curve satisfies the first-order kinetic equation:<sup>16</sup>

$$C_t = C_{\infty}(1 - e^{-kt}), \quad (8)$$

where  $t$  represents the digestion time;  $C_t$  is the reaction concentration at time  $t$ ;  $C_{\infty}$  is the concentration of reactant at end time; and  $k$  is a fitted first-order rate constant.  $C_{\infty}$  and  $k$  were obtained using the Origin 8.0 fitted curve.

### 2.4. Laser scanning confocal microscopy

Ethanol (95%) was used to prepare fluorescein 5-isothiocyanate (FITC) solution and rhodamine B solution with a concentration of 2 mg mL<sup>-1</sup> each. 20  $\mu$ L of each of the above two solutions were taken and simultaneously added into 50 mL of gelatinized starch sample [1% of wheat starch (containing 0.5% gardenia yellow) was dispersed in aqueous solution and gelatinized at 80 °C for 30 min, and the gelatinized starch without gardenia starch was taken as the blank] for dyeing. The mixture was preserved at room temperature for 24 h. The dyed and gelatinized starch samples with and without gardenia yellow (blank) were placed on a glass slide successively, and the starch dyeing conditions were observed under a laser scanning confocal microscope [FV3000, Olympus (China) Co., Ltd., Beijing, China] within 15 min. The excitation wavelengths of FITC and rhodamine B were 488 and 553 nm, respectively.



## 2.5. Dig digestive enzyme activity test of starch

**2.5.1.  $\alpha$ -Amylase activity test.** Phosphate buffer solution (PBS, 0.2 M, pH: 6.8) was used to prepare wheat starch solution (concentration: 1.0 g/100 mL) as the substrate, which was then gelatinized in an 80 °C water bath kettle for 30 min. PBS (0.2 M, pH: 6.8) was also used to prepare gardenia yellow solutions with different concentrations (0.1, 0.3, 0.5, 0.7, and 1.00 mg mL<sup>-1</sup>). Acarbose of the same concentration was taken as the positive control. Then, 250  $\mu$ L of gardenia yellow and acarbose solutions and 250  $\mu$ L of  $\alpha$ -amylase (300 U mL<sup>-1</sup>) dissolved in PBS (0.2 M, pH 6.8) with different concentrations were added into different glass tubes with stoppers. After blending, each glass tube was oscillated in 37 °C thermostatic water bath at 150 rpm for 10 min, and then 500  $\mu$ L of starch solution (concentration: 1.0 g/100 mL) was added. After continuous oscillation of the above mixture in 37 °C water bath at 150 rpm for 10 min, 2.0 mL of DNS color developing agent (28 mM 3,5-dinitrosalicylic acid, 0.6 M potassium sodium tartrate, and 2 M sodium hydroxide) was added to terminate the reaction, and then the reactant was heated in boiling water for 5 min. Its volume was made constant at 25 mL using deionized water after being cooled to room temperature, and the absorbance was determined *via* ultraviolet-visible (UV-vis) spectrophotometer (UV-1600B, Shanghai Mapada Instruments Co., Ltd., Shanghai, China) at 540 nm.<sup>17</sup> The  $\alpha$ -amylase inhibitory activity was measured under different concentrations of gardenia yellow, and the IC<sub>50</sub> value was calculated. The inhibitory effect was calculated using the following formula:

$$\alpha\text{-Amylase inhibition rate (\%)} = \frac{[1 - (A_{\text{sample}} - A_{\text{sample control}})]}{(A_{\text{blank}} - A_{\text{blank control}})} \times 100\%, \quad (9)$$

where  $A_{\text{sample}}$  is the absorbance of mixture of gardenia yellow, substrate, enzyme, and DNS color developing agent;  $A_{\text{sample control}}$  is the absorbance of mixture of gardenia yellow, substrate, and DNS color developing agent, and the enzymatic solution is replaced by PBS;  $A_{\text{blank}}$  is the absorbance of mixture of substrate, enzyme, and DNS color developing agent, and gardenia yellow is replaced by PBS; and  $A_{\text{blank control}}$  is the absorbance of mixture of enzyme-free substrate and DNS color developing agent.

**2.5.2.  $\alpha$ -Glucosidase activity test.**  $\alpha$ -Glucosidase (60 U mL<sup>-1</sup>) and *p*NPG were dissolved in PBS (0.2 M, pH 6.8). Gardenia yellow solutions with different concentrations (0.1, 0.3, 0.5, 0.7, and 1.00 mg mL<sup>-1</sup>) were prepared using PBS (0.2 M, pH 6.8). Acarbose of the same concentration was taken as the positive control. Then, 20  $\mu$ L gardenia yellow solutions with different concentrations of 20  $\mu$ L enzymatic solution were added into a 96-well plate, and the mixture was placed in water bath at 37 °C for 10 min after being blended. Subsequently, 20  $\mu$ L of 3.0 mM *p*NPG substrate solution was added for continuous reaction at 37 °C for 30 min, and 100  $\mu$ L of 0.2 M Na<sub>2</sub>CO<sub>3</sub> solution was immediately added to terminate the reaction. The mixture was then oscillated in a shaking table for 5 min. The absorbance was determined using a 96-well ELISA plate

(Multiskan FC, ThermoFisher Instruments Co., Ltd., Shanghai, China) at 405 nm.<sup>17</sup> The inhibitory effect was calculated using the following formula:

$$\alpha\text{-Glucosidase inhibition rate (\%)} = \frac{[1 - (A_{\text{sample}} - A_{\text{sample control}})]}{(A_{\text{blank}} - A_{\text{blank control}})} \times 100\%, \quad (10)$$

where  $A_{\text{sample}}$  is the absorbance of mixture of gardenia yellow, substrate, enzyme, and DNS color developing agent;  $A_{\text{sample control}}$  is the absorbance of mixture of gardenia yellow, substrate, and DNS color developing agent, and the enzymatic solution is replaced by PBS;  $A_{\text{blank}}$  is the absorbance of mixture of substrate, enzyme, and DNS color developing agent, and gardenia yellow is replaced by PBS; and  $A_{\text{blank control}}$  is the absorbance of mixture of enzyme-free substrate and DNS color developing agent.

## 2.6. Inhibition kinetic test of starch digestive enzymes

**2.6.1.  $\alpha$ -Amylase inhibition kinetic test.** The inhibitory mode of gardenia yellow for  $\alpha$ -amylase was determined using Michaelis–Menton and Lineweaver–Burk equations.<sup>18</sup> Using the  $\alpha$ -amylase activity test as reference, the wheat starch solution was taken as the substrate in the test process, dissolved in PBS (0.2 M, pH 6.8), and gelatinized in an 80 °C water bath kettle for 30 min. When the gelatinized starch solution was diluted, its concentration reached 0.5%, 1.0%, 1.5%, and 2.0% (W/V). The concentrations of gardenia yellow solution were 0.5 and 0.7 mg mL<sup>-1</sup>. One test tube of sample with each concentration was taken out every other 5 min, and 2 mL of DNS color developing agent was added. The reactant was then heated in boiling water bath for 5 min and cooled to room temperature with a constant volume of 25 mL. The absorbance was determined using the UV-vis spectrophotometer at 540 nm.

The Michaelis–Menten equation is as follows:

$$V = V_{\text{max}} \times \frac{[S]}{K_m + [S]} \quad (11)$$

The Lineweaver–Burk equation is as follows:

$$\frac{1}{V} = \frac{1}{V_{\text{max}}} + \frac{K_m}{V_{\text{max}}} \times \frac{1}{[S]} \quad (12)$$

Double-reciprocal straight lines under different  $I$  values were firstly drawn, and then the slope for one-time plotting under different  $I$  values was obtained.  $K_{ic}$  was obtained by plotting with  $I$  and slope. The equation is as below:

$$\text{Slope} = \frac{K_m}{V_{\text{max}}} + \frac{K_m}{V_{\text{max}} K_{ic}} I \quad (13)$$

$$Y\text{-intercept} = \frac{1}{V'_{\text{max}}} = \frac{1}{V_{\text{max}}} + \frac{1}{\alpha K_{iu} V_{\text{max}}} I \quad (14)$$

The graph of slope or  $Y$ -intercept and  $I$  was drawn once again and linearly fitted, where  $V$  is the initial reaction velocity;  $S$  is



the substrate concentration;  $V_{\max}$  is the maximum initial reaction velocity;  $I$  is the inhibitor concentration;  $\alpha$  is the apparent coefficient;  $K_m$  is the Michaelis constant;  $K_{ic}$  is the competitive inhibition constant;  $K_{iu}$  is the noncompetitive inhibition constant.

**2.6.2.  $\alpha$ -Glucosidase inhibition kinetic test.** The inhibition kinetic determination method of  $\alpha$ -glucosidase was the same as that of  $\alpha$ -amylase inhibition kinetic test. The concentrations of gardenia yellow solution were still 0.5 and 0.7 mg mL<sup>-1</sup>, and the concentration range of pNPG solution as the substrate was set as 0.5–5.0 mM. The inhibition kinetic study was conducted using the method introduced in the  $\alpha$ -glucosidase activity test as reference. The ELISA plate was taken out every other 5 min and added with 100  $\mu$ L of 0.2 M sodium carbonate solution to terminate the reaction, and the absorbance at 405 nm was determined using the 96-well ELISA kit (Multiskan FC, Samer Feishier Instrument Co., Ltd., Shanghai, China). The inhibitory mode of gardenia yellow for  $\alpha$ -glucosidase was determined *via* Michaelis–Menton and Lineweaver–Burk equations, and the inhibition type was acquired. The concrete calculation process was the same as the  $\alpha$ -amylase inhibition kinetic test.

## 2.7. Inhibition kinetic test of starch digestive enzymes

**2.7.1. Analysis of  $\alpha$ -amylase fluorescence quenching.** The fluorescence quenching spectra of gardenia yellow on  $\alpha$ -amylase were tested using a fluorospectrophotometer (G9800A, Agilent Technological Co., Ltd., Malaysia). The gardenia yellow solutions with concentrations of 0.025, 0.1, 0.3, 0.5, 0.7, and 1 mg mL<sup>-1</sup> was prepared in PBS.  $\alpha$ -Amylase (300 U mL<sup>-1</sup>) was dissolved into the PBS (pH: 6.8), 0.2 mL of gardenia yellow with different concentrations was added into 3 mL of  $\alpha$ -amylase solution, and the volume of the mixture was made constant at 10 mL after vortex oscillation for 2 min. The mixture was oscillated at constant temperature under 30 °C and 37 °C water batch conditions for 30 min. The equivalent amount of PBS was taken as the blank reference, the excitation wavelength was 278 nm, the emission wavelength was 290 nm, the slit width was 5 nm, and the fluorescence emission spectra were scanned at the wavelength range of 290–500 nm. The fluorescence quenching was described through the Stern–Volmer equation as follows:

$$\frac{F_0}{F} = 1 + K_{SV}[Q] \quad (15)$$

$$K_{SV} = K_q\tau_0 \quad (16)$$

where  $F_0$  and  $F$  represent the fluorescence intensities of the fluorescent substance with and without the existence of quenching agent, respectively;  $K_{SV}$  and  $K_q$  are the Stern–Volmer quenching constant and the bimolecular fluorescence quenching rate constant controlled by the diffusion process, respectively;  $[Q]$  is the concentration of quenching agent; and  $\tau_0$  is the average life of fluorescence molecule (the  $\tau_0$  of  $\alpha$ -amylase is 2.97 ns, and that of  $\alpha$ -glucosidase is  $10^{-8}$  s).

**2.7.2. Analysis of  $\alpha$ -glucosidase fluorescence quenching.** The fluorescence spectrometry of  $\alpha$ -glucosidase was the same as

the analysis of  $\alpha$ -amylase fluorescence quenching, where the activity of  $\alpha$ -glucosidase was 180 U mL<sup>-1</sup>, the excitation wavelength was 278 nm, the slit width was 5 nm, and the fluorescence emission spectra were scanned within the wavelength range of 290–450 nm.

**2.7.3. Thermodynamic parameter assessment.** Micro-molecules and biological macromolecules could interact through hydrophobic bond, electrostatic attraction, van der Waals force, and H bond. The thermodynamic parameters of the standard enthalpy change  $\Delta H$  and standard entropy change  $\Delta S$  could be determined using van 't Hoff equation, and the results from van 't Hoff plots were based on two temperatures as follows:<sup>19</sup>

$$\ln K_a = -\frac{\Delta H}{RT} + \frac{\Delta S}{R} \quad (17)$$

where  $R$  is the atmospheric constant with the value of 8.314 J mol<sup>-1</sup> K<sup>-1</sup>,  $T$  is the reaction temperature (303 K and 310 K), and  $K_a$  is the binding constant. The free energy  $\Delta G$  is calculated by eqn (18) as follows:

$$\Delta G = \Delta H - T\Delta S, \quad (18)$$

The  $\Delta H$  and  $\Delta S$  values were calculated from the slope and intercept of the linear relation curve between  $\ln K_a$  and  $1/T$ .

**2.7.4. Secondary structure test of starch digestive enzymes.** By reference to the method of Wu,<sup>20</sup> a circular dichroism chromatograph (MOS-450, Bio-Logic Company, France) was used to determine the secondary structures of  $\alpha$ -amylase and  $\alpha$ -glucosidase with and without the existence of gardenia yellow. First,  $\alpha$ -amylase and  $\alpha$ -glucosidase were dissolved in phosphate buffer (0.2 M, pH of 6.8, containing 10% DMSO) and then reacted with gardenia yellow at 37 °C for 30 min. The phosphate solution and gardenia yellow solution were taken as the blank, the circular dichroism (CD) spectrogram at 190–250 nm was scanned, and the parameters were as follows: temperature (37 °C), bandwidth (1 nm), and spectral resolution (30 nm min<sup>-1</sup>). The CD spectral data of  $\alpha$ -amylase and  $\alpha$ -glucosidase were processed *via* Origin. The contents of secondary structures ( $\alpha$ -helix,  $\beta$ -sheet,  $\beta$ -turn, and random coil) of digestive enzymes were calculated online by using SELCON3 program.

## 2.8. Statistical analysis

All data were analyzed on SPSS version 22 statistical software, and the results were expressed in mean  $\pm$  standard deviation ( $n = 3$ ). The significance of difference was tested through the Duncan test method, and  $P < 0.05$  indicated statistically significant difference.

# 3. Results and discussion

## 3.1. Effects of gardenia yellow on *in vitro* starch digestion

The hydrolysis rates of wheat starch added with 0%, 0.1%, 0.5%, 1%, and 2% of gardenia yellow at 20 min were 68.58%, 66.57%, 65.01%, 63.45%, and 60.54%, respectively, and those at 180 min were 81.98%, 83.76%, 71.26%, 73.27%, and 64.12%, respectively. As shown in Fig. 1, the slope of curve and hydrolysis rate



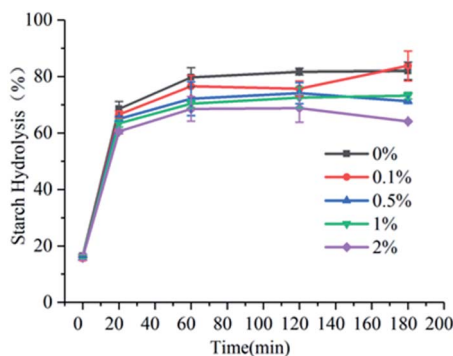


Fig. 1 Influence of content of gardenia yellow on starch digestion.

reached the peak within 0–20 min, and after 180 min, the sample tended to a hydrolytic equilibrium. According to the study of Zang *et al.*, amylolysis satisfies the first-order reaction kinetic equation.<sup>10</sup> Table 2 shows that with the increase in the concentration of gardenia yellow, the equilibrium concentration of wheat starch was always lower than that in the blank group, and as the content of gardenia yellow was further increased, the equilibrium concentration presented a declining trend, indicating that gardenia yellow could effectively reduce the amylolysis rate and slow down the starch digestion.

In general, white bread has been used for reference in the *in vitro* studies of GI value (GI value of white bread = 100); low-, medium-, and high-GI food standards are defined as  $GI < 60$ ,  $GI = 60–85$ , and  $GI > 85$ , respectively,<sup>21</sup> which, however, obviously could not be used to define the change in starch digestion caused by gardenia yellow. Therefore, the complete hydrolysis of wheat starch without gardenia yellow was taken for reference, and a comparison was made to obtain the change in GI value

after the addition of gardenia yellow. As seen in Table 2, after the gardenia yellow of different concentrations was added, the GI value of wheat starch was apparently reduced, indicating that gardenia yellow could effectively reduce the GI value and facilitate the stabilization of blood glucose.

Rapidly digestible starch (RDS) refers to starch rapidly digested within 20 min, could lead to a sharp increase in blood glucose and insulin, whereas the digestion time of slowly digestible starch (SDS) is generally controlled within 20–120 min. SDS could slow down the elevation of postprandial blood glucose, provide slow and stable glucose release, and contribute to the stabilization of blood glucose. Resistant starch (RS) is difficult to be digested and utilized, with digestion time of longer than 120 min. It could cause a sudden increase in the blood glucose level and give rise to diabetes and coronary heart diseases. The complete digestion rate of SDS in small intestine is much slower than that of RDS. Thus, it could improve the satiety and relieve diabetic symptoms. RS is a component that could avoid being digested by the upper digestive tract, and it is fermented through the microflora. Similar with dietary fiber in large intestine, RS could intervene in metabolic syndrome and reduce the morbidity of colorectal carcinoma. By virtue of its beneficial physiological actions, RS has been considered as an ideal good composition. Thus, the three types of starch could trigger different *in vivo* glycemic reactions.<sup>22,23</sup> As seen in Table 1, with the increase in the content of gardenia yellow, RDS, SDS, and RS all experienced significant changes, among which RDS was decreased by 8.56%, while RS was increased by 23.7% of the same growth percentage as the content of gardenia yellow. This finding was mainly the result of gardenia yellow-starch and gardenia yellow-starch digestive enzyme joint actions. On the one hand, the interaction between gardenia yellow and starch may enlarge the contact area between starch

Table 1 Influence of content of gardenia yellow on *in vitro* wheat starch digestion (Englyst method)<sup>a</sup>

Content of gardenia yellow/%	0	0.1	0.5	1.0	2.0
RDS content/%	53.44 ± 2.49 <sup>a</sup>	51.79 ± 1.46 <sup>b</sup>	49.79 ± 0.45 <sup>b</sup>	47.85 ± 0.78 <sup>b</sup>	44.88 ± 1.56 <sup>c</sup>
SDS content/%	12.95 ± 1.69 <sup>a</sup>	9.68 ± 1.31 <sup>b</sup>	9.97 ± 0.9 <sup>b</sup>	7.26 ± 0.16 <sup>c</sup>	8.48 ± 1.11 <sup>bc</sup>
RS content/%	33.61 ± 1.44 <sup>c</sup>	43.07 ± 5.66 <sup>b</sup>	44.41 ± 6.43 <sup>ab</sup>	46.64 ± 3.17 <sup>ab</sup>	57.36 ± 5.61 <sup>a</sup>

<sup>a</sup> Each datum is expressed by mean ± standard deviation obtained after three times of measurement; the significance of difference was tested through the Duncan test method; different alphabets in each column mean significant differences ( $P < 0.05$ ).

Table 2 Influences of content of gardenia yellow on wheat starch hydrolysis model parameters and glycemic index (Goni method)<sup>a</sup>

Content of gardenia yellow/%	$C_{\infty}/\%$	$k/\text{min}$	$R$	HI	GI
0	81.01 ± 4.56	0.091 ± 0.036	0.9166	100.00 <sup>a</sup>	94.61 <sup>a</sup>
0.1	77.40 ± 5.03	0.089 ± 0.040	0.9115	95.19 ± 0.03 <sup>b</sup>	91.97 ± 0.02 <sup>b</sup>
0.5	68.88 ± 5.70	0.121 ± 0.100	0.9007	88.01 ± 0.30 <sup>c</sup>	88.13 ± 0.17 <sup>c</sup>
1.0	70.29 ± 4.86	0.105 ± 0.06	0.9162	88.25 ± 0.89 <sup>c</sup>	88.16 ± 0.49
2.0	65.46 ± 4.70	0.120 ± 0.08	0.8414	83.12 ± 0.14 <sup>d</sup>	85.34 ± 0.08 <sup>d</sup>

<sup>a</sup> Each datum is expressed by mean ± standard deviation obtained after three times of measurement; the significance of difference was tested through the Duncan test method; different alphabets in each column indicate significant differences ( $P < 0.05$ ).



and enzyme and accelerate the starch digestion. On the other hand, the activity of starch digestive enzyme was inhibited, and the starch digestion rate decreased after the interaction with starch digestive enzymes. This finding was in accordance with the influence result of flavonoids in lotus leaves on starch digestion obtained by Wang.<sup>23</sup>

### 3.2. Laser confocal scanning

As shown in Fig. 2, the wheat starch could be dyed very well. Thus, FITC was a fluorochrome suitable for observing the position of gelatinized starch, but due to the loss of hydrophobic zone, rhodamine B could not realize intense dyeing in gelatinized starch.<sup>24</sup> Rhodamine B and FITC could serve as the dyestuffs of gardenia yellow and gelatinized wheat starch, respectively. FITC presented green fluorescence, indicating that the gelatinized wheat starch bound to FITC to generate green fluorescence, while gardenia yellow bound to rhodamine B to develop red color (arrows in Fig. 2B). Fig. 2 shows that the wheat starch contained two types of starch grains, namely, large disciform a-type grains (approximately 20–40  $\mu\text{m}$ ) and small circular b-type grains (2–5  $\mu\text{m}$ ).<sup>25</sup> As illustrated in Fig. 2, the dilatant starch grains tended to be aggregated, while most gardenia yellow was dispersed outside the starch grains. In addition, gardenia yellow may interact with the amylose leaching out. The partial color formed by binding was yellow and not red, which may be ascribed to the superposition result after starch and gardenia yellow were dyed. The above phenomenon could be explained using the co-regionalization of gardenia yellow and amylose, that is, gardenia yellow and the leaching amylose jointly formed a network structure.<sup>23,26</sup>

### 3.3. $\alpha$ -Amylase and $\alpha$ -glucosidase inhibition

As shown in Fig. 3, gardenia yellow and acarbose exerted obvious inhibitory effects on  $\alpha$ -amylase and  $\alpha$ -glucosidase. With the increase in the concentrations of acarbose and gardenia yellow, their inhibitory effects on  $\alpha$ -amylase became more obvious than before. Acarbose reached the inhibition rate of 45.74% under the concentration of 1.0  $\text{mg mL}^{-1}$  and gardenia yellow reached 26.71% under the concentration of 1.0  $\text{mg mL}^{-1}$ . Through the SPSS data processing, the  $\text{IC}_{50}$  values of acarbose and gardenia yellow for  $\alpha$ -amylase were found to be 1.270 and 2.973  $\text{mg mL}^{-1}$ , respectively. Similar with the inhibitory effect

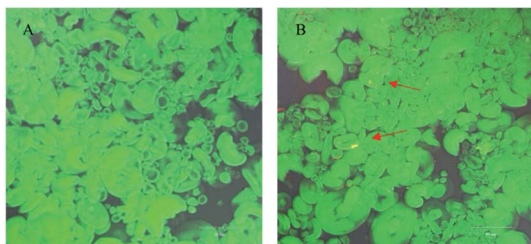


Fig. 2 Laser confocal scanning graphs of wheat starch (graph (A) is blank, and graph (B) shows the condition after addition of 0.5% gardenia yellow). \*Note: arrows indicate that rhodamine B binds to gardenia yellow and thus becomes red.

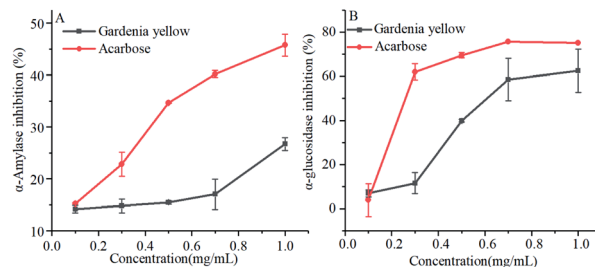


Fig. 3 Inhibitory effect of gardenia yellow on  $\alpha$ -amylase (A) and  $\alpha$ -glucosidase (B).

on  $\alpha$ -amylase,  $\alpha$ -glucosidase could be inhibited by gardenia yellow and acarbose, and the inhibitory effect depended on the dosage. The inhibition rates of gardenia yellow and acarbose for  $\alpha$ -glucosidase were 62.46% and 74.77% under the concentration of 1.0  $\text{mg mL}^{-1}$ , respectively, and the  $\text{IC}_{50}$  values were 0.677 and 0.171  $\text{mg mL}^{-1}$ , respectively. The results showed that the inhibitory effect of gardenia yellow on  $\alpha$ -glucosidase activity was greater than that on  $\alpha$ -amylase activity, that mean it is a mild  $\alpha$ -amylase inhibitor but a strong  $\alpha$ -glucosidase inhibitor, which was similar with polyphenols.<sup>17</sup> In addition, acarbose exerted more outstanding inhibitory effects on  $\alpha$ -amylase and  $\alpha$ -glucosidase than gardenia yellow. However, as a natural plant extract, gardenia yellow integrates various merits, such as usage safety, and it could effectively prevent phenomena such as abdominal distension, which may be generated when acarbose is used.<sup>27,28</sup>

### 3.4. Kinetics of gardenia yellow inhibiting $\alpha$ -amylase and $\alpha$ -glucosidase activities

In the inhibition kinetic analysis, the competitive inhibition constant  $K_{ic}$  is a dissociation constant of inhibitor–enzyme compound. Therefore,  $1/K_{ic}$  represents the association constant of inhibitor and enzyme; low  $K_{ic}$  value means high affinity between inhibitor and enzymatic active site.<sup>29</sup> As seen in Table 3, the  $K_{ic}$  of gardenia yellow for  $\alpha$ -amylase was greater than that for  $\alpha$ -glucosidase, suggesting higher affinity of gardenia yellow for  $\alpha$ -glucosidase.

Fig. 4 and Table 3 show that under increasing concentration of gardenia yellow and unchanged vertical intercept, that is,  $V_{\text{max}}$  was unchanged, the horizontal intercept was reduced, that is, the Michaelis constant was increased. The inhibition type of gardenia yellow for  $\alpha$ -amylase and  $\alpha$ -glucosidase was competitive inhibition, which mean gardenia yellow bound to the active centers of  $\alpha$ -amylase and  $\alpha$ -glucosidase to generate the influence on enzymatic activity. This type was similar with the inhibition of polyphenols for digestive enzymes.<sup>17,30</sup> However, some phenolic acids were mixed inhibitory effects on  $\alpha$ -amylase and  $\alpha$ -glucosidase, such as naked oat phenolic acid.<sup>31</sup>

### 3.5. Fluorescence quenching effect of gardenia yellow on $\alpha$ -amylase and $\alpha$ -glucosidase

Under the excitation wavelength of 278 nm, the maximum emission wavelength of  $\alpha$ -amylase was around 346 nm, and that of  $\alpha$ -glucosidase was 341 nm. Under different temperatures and



Table 3 Influence of gardenia yellow on inhibition kinetic parameters of  $\alpha$ -amylase and  $\alpha$ -glucosidase<sup>a</sup>

Digestive enzyme	$K_m$ ( $10^{-2}$ mg mL <sup>-1</sup> )			$V_{max}$ ( $10^{-2}$ mg mL <sup>-1</sup> min <sup>-1</sup> )	Inhibition type	$K_{ic}$ (mg mL <sup>-1</sup> )
	A	B	C			
$\alpha$ -Amylase	2.63	3.30	3.93	0.52	Competitive inhibition	1.47
$\alpha$ -Glucosidase	1.44	2.16	3.22	3.11	Competitive inhibition	0.58

<sup>a</sup> A, B, and C represent the concentrations of gardenia yellow at 0.0, 0.5, and 0.7 mg mL<sup>-1</sup>, respectively.

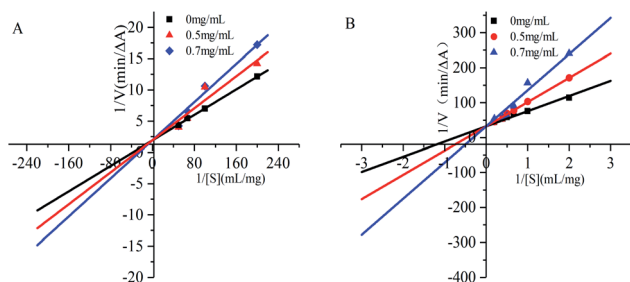


Fig. 4 Lineweaver–Burk curves about inhibitory effects of gardenia yellow on  $\alpha$ -amylase (A) and  $\alpha$ -glucosidase (B).

a certain wavelength range, the fluorescence intensities of  $\alpha$ -amylase and  $\alpha$ -glucosidase were reduced to different degrees with the increase in the concentration of gardenia yellow, namely, the fluorescence quenching phenomenon. In addition, Fig. 5 and 6 show that the wavelengths at the maximum emission peaks of  $\alpha$ -amylase and  $\alpha$ -glucosidase experienced red shifts, indicating that the addition of gardenia yellow reduced the microenvironment hydrophobicity of fluorescence chromophoric groups of  $\alpha$ -amylase and  $\alpha$ -glucosidase, with enhanced hydrophilia and peptide chain extensibility. The fluorescence analysis provided information regarding the molecular environment nearby chromophores. The reduction in the intrinsic fluorescence intensity of protein is called quenching, which has two different mechanisms, dynamic quenching and static quenching. When the excited-state fluorophores contact other molecules (quenching agent) in the solution and experience inactivation, collision quenching

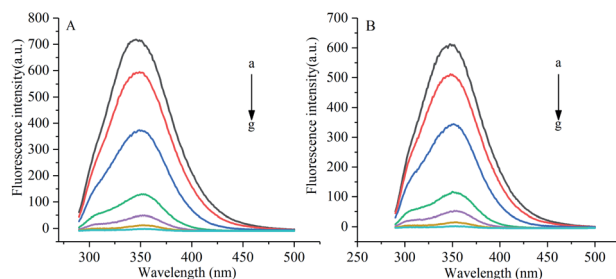


Fig. 5 Influence of gardenia yellow on fluorescence spectrogram of  $\alpha$ -amylase ((A) and (B) show the fluorescence spectra of  $\alpha$ -amylase at 30 °C and 37 °C, respectively). \*Note: a–g denotes the concentrations of gardenia yellow at 0, 0.025, 0.1, 0.3, 0.5, 0.7, and 1 mg mL<sup>-1</sup>, respectively.

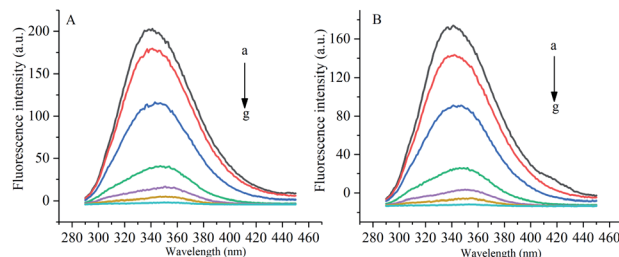


Fig. 6 Influence of gardenia yellow on fluorescence spectrograms of  $\alpha$ -glucosidase ((A) and (B) show the fluorescence spectrograms of at 30 °C and 37 °C, respectively).

(dynamic quenching) then occurs, and when they form a non-fluorescent complex with the quenching agent, static quenching then takes place.<sup>32</sup>

As shown in Fig. 7, the Stern–Volmer curves of gardenia yellow for  $\alpha$ -amylase and  $\alpha$ -glucosidase were bent towards the axis y. In general, the linear Stern–Volmer curve indicates that a type of fluorophores in the protein interact with the quenching agent in the same manner, in which only one quenching mechanism (dynamic or static) exists. However, the positive deviation of equation could be usually observed under a high quenching degree. Under this circumstance,  $F_0/F[Q]$  describes an upward curve, namely, the depression towards the axis y. In general, upward bending suggests that several mechanisms take charge of the quenching effect of fluorophores in the protein, including dynamic quenching and static quenching, or an “action scope” exists, that is, apparent static quenching.<sup>32,33</sup> The modified Stern–Volmer equation used to describe this circumstance is as follows:<sup>30</sup>

$$\frac{F_0}{F} = e^{(K_{SV}[Q])} \quad (19)$$

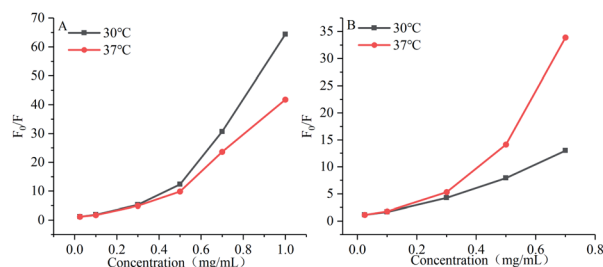


Fig. 7 Influences of gardenia yellow on fluorescence quenching Stern–Volmer graphs of  $\alpha$ -amylase (A) and  $\alpha$ -glucosidase (B).



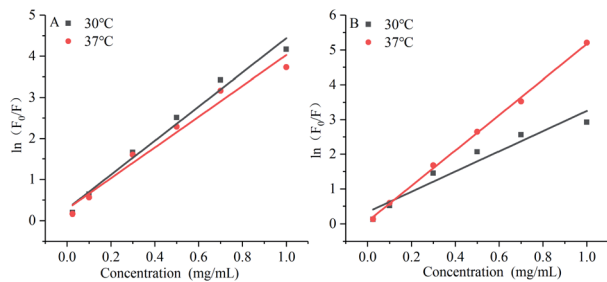


Fig. 8 Influences of gardenia yellow on modified fluorescence quenching Stern–Volmer charts of  $\alpha$ -amylase (A) and  $\alpha$ -glucosidase (B).

Natural logarithms were taken from both sides of this equation to draw the chart of  $\ln(F_0/F)$  and  $[Q]$ , a straight line was obtained, and the slope of this line refers to the apparent static constant  $K_{SV}$  as below:

$$\ln \frac{F_0}{F} = K_{SV}[Q] \quad (20)$$

The modified Stern–Volmer diagram is shown in Fig. 8.

The maximum dynamic quenching constant of biopolymers in different quenching agents is always  $2 \times 10^{10} \text{ M}^{-1} \text{ S}^{-1}$ . Table 4 shows that the fluorescence quenching constant of gardenia yellow for  $\alpha$ -amylase and  $\alpha$ -glucosidase was much greater than  $2 \times 10^{10} \text{ M}^{-1} \text{ S}^{-1}$ , indicating that gardenia yellow showed greater affinity with them. The main quenching mechanism was static quenching, the quenching constant for  $\alpha$ -glucosidase was greater than that for  $\alpha$ -amylase at 37 °C, which, to some extent, proved that gardenia yellow had stronger affinity and closer interaction with  $\alpha$ -glucosidase.<sup>34,35</sup>

### 3.6. Influences of gardenia yellow on binding constant and number of binding sites of $\alpha$ -amylase and $\alpha$ -glucosidase

The binding constant  $K_a$  and number of binding site  $n$  of gardenia yellow for  $\alpha$ -amylase and  $\alpha$ -glucosidase are shown in Table 5. The binding constant and number of binding sites for both starch digestive enzymes were changed to some extent, reflecting that temperature was an important factor in the influence of gardenia yellow on the two enzymes. As the temperature was elevated, the value of  $\alpha$ -amylase was reduced, indicating that gardenia yellow had a declining affinity with  $\alpha$ -amylase, but the affinity of glucosidase with gardenia yellow was gradually enhanced (30–37 °C). The value of  $n$  was slightly greater than 1, indicating that gardenia yellow exerted the effect on the two digestive enzymes at over one binding site or at binding sites of over one type.<sup>35</sup>

Table 5 Influences of gardenia yellow on binding constant and number of binding sites of  $\alpha$ -amylase and  $\alpha$ -glucosidase

Digestive enzyme	Temperature/°C	$K_a$	$n$	$R^2$
$\alpha$ -Amylase	30	473.77	1.53	0.9701
	37	320.92	1.48	0.9797
$\alpha$ -Glucosidase	30	146.02	1.34	0.9968
	37	1198.89	1.80	0.9449

Table 6 Influences of gardenia yellow on thermodynamic parameters of  $\alpha$ -amylase and  $\alpha$ -glucosidase

Starch digestive enzyme	Temperature/°C	$\Delta H$ (kJ mol <sup>-1</sup> )	$\Delta S$ (kJ mol <sup>-1</sup> )	$\Delta G$ (kJ mol <sup>-1</sup> )
$\alpha$ -Amylase	30	-43.22	-34.01	-32.92
	37			-32.68
$\alpha$ -Glucosidase	30	234.882	0.874	-29.956
	37			-35.075

### 3.7. Influences of gardenia yellow on the thermodynamic parameters of $\alpha$ -amylase and $\alpha$ -glucosidase

Based on the abovementioned interactions between gardenia yellow and starch digestive enzymes, thermodynamic analysis was further conducted to determine the primary causes for the interactions. In general, four interaction forces exist between small ligands and biomolecules, namely, hydrogen bond, vdW force, hydrophobic interaction, and electrostatic interaction. The results in Table 6 showed that when the  $\Delta G$  value was negative, the binding process between gardenia yellow and starch digestive enzymes ( $\alpha$ -amylase and  $\alpha$ -glucosidase) was spontaneous.<sup>36</sup> In addition, the calculated  $\Delta H$  and  $\Delta S$  values for  $\alpha$ -amylase were -43.22 and -34.01 kJ mol<sup>-1</sup>, respectively, and those for  $\alpha$ -glucosidase were 234.88 and 0.87 kJ mol<sup>-1</sup>,

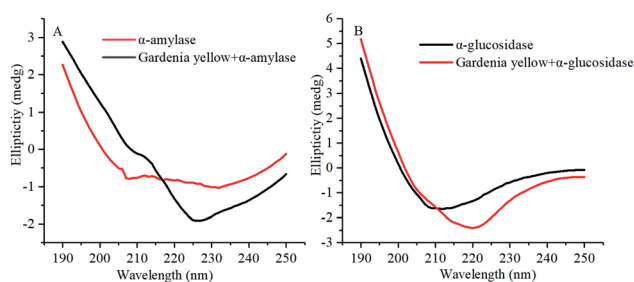


Fig. 9 Influence of gardenia yellow on CD spectrograms of  $\alpha$ -amylase (A) and  $\alpha$ -glucosidase (B).

Table 4 Influences of gardenia yellow on Stern–Volmer equations and equation parameters of  $\alpha$ -amylase and  $\alpha$ -glucosidase

Digestive enzyme	Temperature/°C	Stern–Volmer equation	$R^2$	$K_{SV}$ (10 <sup>3</sup> /M)	$K_q$ (10 <sup>11</sup> M S <sup>-1</sup> )
$\alpha$ -Amylase	30	$\ln F_0/F = 4.15 \times 10^3 [Q] + 0.2817$	0.97829	$4.15 \pm 0.28$	1.40
	37	$\ln F_0/F = 3.75 \times 10^3 [Q] + 0.2779$	0.96719	$3.75 \pm 0.30$	1.26
$\alpha$ -Glucosidase	30	$\ln F_0/F = 2.92 \times 10^3 [Q] + 0.3328$	0.92702	$2.92 \pm 0.36$	2.92
	37	$\ln F_0/F = 5.10 \times 10^3 [Q] + 0.0650$	0.99827	$5.10 \pm 0.09$	5.10





Table 7 Influence of gardenia yellow on secondary structures of  $\alpha$ -amylase and  $\alpha$ -glucosidase

Starch digestive enzyme	Concentration of gardenia yellow (mg mL <sup>-1</sup> )	Contents of secondary structures in $\alpha$ -amylase and $\alpha$ -glucosidase (%)			
		$\alpha$ -Helix/%	$\beta$ -Sheet/%	$\beta$ -Turn/%	Random coil/%
$\alpha$ -Amylase	0	29.2	37.9	16.9	24.9
	0.4	2.30	42.8	21.9	32.1
$\alpha$ -Glucosidase	0	18.8	30.4	16.3	53.6
	0.4	2.6	50.0	23.4	23.8

respectively. vdW force was the main force driving the interaction between gardenia yellow and  $\alpha$ -glucosidase, while hydrophobic interaction was the main force driving the interaction between gardenia yellow and  $\alpha$ -glucosidase.<sup>37</sup>

### 3.8. Effects of gardenia yellow on the secondary structures of $\alpha$ -amylase and $\alpha$ -glucosidase

The CD spectrograms of  $\alpha$ -amylase and  $\alpha$ -glucosidase with and without gardenia yellow are shown in Fig. 9. A negative band was found within 210–220 nm. Under the action of gardenia yellow, negative bands were obviously observed in the CD spectrograms of  $\alpha$ -amylase and  $\alpha$ -glucosidase, indicating the changes in their secondary structures.  $\alpha$ -Helix was mainly characterized by the electron transfer of  $\alpha$ -helical bond caused by the electron transfer of  $n \rightarrow \pi^*$  and  $\pi \rightarrow \pi^*$  at 210 and 222 nm.<sup>38</sup> The changes in the ovality of negative bands showed that with the addition of gardenia yellow, the contents of  $\alpha$ -helix in both enzymes were changed as gardenia yellow interacted with them, thus leading to changes in their conformations.

Table 7 lists the proportions of secondary structures in  $\alpha$ -amylase and  $\alpha$ -glucosidase. After gardenia yellow was added, the content of  $\alpha$ -helix in  $\alpha$ -amylase decreased from 29.2% to 2.30%, while the contents of  $\beta$ -sheet,  $\beta$ -turn, and random coil increased from 37.9%, 16.9%, and 24.9% to 42.8%, 21.9%, and 32.1%, respectively. The contents of  $\alpha$ -helix and random coil in  $\alpha$ -glucosidase decreased from 18.8% and 53.6% to 2.6% and 23.8%, respectively, while the contents of  $\beta$ -sheet and  $\beta$ -turn increased from 50.0% and 23.4%, respectively. By combining the synchronous fluorescence spectroscopy and thermodynamic parameter analysis, a conclusion could be made that the binding of gardenia yellow to  $\alpha$ -amylase and  $\alpha$ -glucosidase may damage the hydrogen bond structure of the enzymes and change their secondary structures, thus hindering the formation of an active center or preventing the substrate binding and leading to the change in enzymatic activity.<sup>19</sup>

According to fluorescence quenching, synchronous spectroscopy, and circular dichroism spectral analysis, during the action process of gardenia yellow on starch digestive enzymes, the binding distances  $r$  of gardenia yellow to  $\alpha$ -amylase and  $\alpha$ -glucosidase was 4.77 and 5.19 nm, respectively, smaller than 8 nm. Gardenia yellow may penetrate into the starch digestive enzymes. Given the extensibility of spatial structure of gardenia yellow and its polyhydroxy structure, the peptide chains of starch digestive enzymes were extended, the polarity of amino acid residues was then changed, and the secondary structures of  $\alpha$ -amylase and  $\alpha$ -glucosidase were changed by the hydrogen

bond and hydrophobic interaction. As a result, the active sites and spatial structures of both enzymes were altered, thus resulting in their activity degradation.

## 4. Conclusion

Gardenia yellow could interact with wheat starch and affect its physiochemical properties and digestion characteristics. Furthermore, it could interact with amylose leaching out of wheat starch and play a significant role in its physiochemical properties. After 2% gardenia yellow was added, the RS and SDS contents in wheat starch significantly increased ( $P < 0.05$ ), while the GI and HI values were obviously reduced. Gardenia yellow could interact with starch digestive enzymes ( $\alpha$ -amylase and  $\alpha$ -glucosidase) and generate competitive inhibition. It also showed higher affinity to  $\alpha$ -glucosidase than to  $\alpha$ -amylase. Moreover, gardenia yellow could spontaneously interact the with catalytic sites of  $\alpha$ -amylase and  $\alpha$ -glucosidase, affect their secondary structures through vdW force and hydrophobic interaction, and reduce their catalytic abilities to inhibit the digestion process of wheat starch. In short, gardenia yellow may play a significant role in stabilizing the blood glucose level in human body, thereby laying a theoretical foundation for screening inhibitors for starch digestive enzymes and developing functional foods for diabetics. However, sufficient scientific evidence from pre-clinical and clinical trials must be done before the application of gardenia yellow in the treatment of diabetes in the future.

## Abbreviations

WHO	World Health Organization
<i>p</i> NPG	<i>p</i> -Nitrophenyl- $\alpha$ -D-glucopyranoside
DNS	3,5-Dinitrosalicylic acid
RDS	Rapid digestive starch
SDS	Slow digestive starch
RS	Resistant starch
FITC	5-Isothiocyanate
UV-vis	Ultraviolet-visible
PBS	Phosphate buffer solution
vdW	van der Waals
CD	Circular dichroism
HI	Hydrolysis index
GI	Glycemic index



## Conflicts of interest

The authors declare no competing financial interest.

## Acknowledgements

This study received financial support from the National Natural Science Foundation of China (No. 31801584, No. 32001703), Henan Natural Science Foundation (No. 182300410079), and the High-Level Talents Foundation of Henan University of Technology (2020BS063).

## References

- 1 J. G. Chen, S. F. Wu, Q. F. Zhang, Z. P. Yin and L. Zhang, *Int. J. Biol. Macromol.*, 2020, **143**, 696–703.
- 2 J. P. Antonio, R. A. Sarmento and J. C. de Almeida, *J. Acad. Nutr. Diet.*, 2019, **119**, 652–658.
- 3 V. M. Butardo Jr and N. Sreenivasulu, *Int. Rev. Cell Mol. Biol.*, 2016, **323**, 31–70.
- 4 R. Azizi, E. Capuano, A. Nasirpour, N. Pellegrini, M.-T. Golmakani, S. M. H. Hosseini and A. Farahnaky, *Food Hydrocolloids*, 2019, **95**, 358–366.
- 5 M. R. Toutounji, A. Farahnaky, A. B. Santhakumar, P. Oli, V. M. Butardo Jr and C. L. Blanchard, *Trends Food Sci. Technol.*, 2019, **88**, 10–22.
- 6 G. Chi, Y. Qi, J. Li, L. Wang and J. Hu, *J. Inorg. Biochem.*, 2019, **193**, 173–179.
- 7 A. Gupta, T. Behl and M. Sachdeva, *Obesity Medicine*, 2020, **17**, 100183.
- 8 C. I. Chukwuma, M. G. Matsabisa, M. A. Ibrahim, O. L. Erukainure, M. H. Chabalala and M. S. Islam, *J. Ethnopharmacol.*, 2019, **235**, 329–360.
- 9 B. L. Furman, M. Candasamy, S. K. Bhattamisra and S. K. Veettil, *J. Ethnopharmacol.*, 2020, **247**, 112264.
- 10 C. X. Zang, X. Q. Bao, L. Li, H. Y. Yang, L. Wang, Y. Yu, X. L. Wang, X. S. Yao and D. Zhang, *Am. J. Chin. Med.*, 2018, **46**, 389–405.
- 11 F. Zhang, Y. H. Wei, Y. T. Duan, Y. S. Zhao, L. L. Xi, Z. Rao, J. P. Zhang, G. Q. Zhang and X. A. Wu, *Chin. Herb. Med.*, 2018, **10**, 431–436.
- 12 H. Zhang, Q. Lai, Y. Li, Y. Liu and M. Yang, *J. Ethnopharmacol.*, 2017, **196**, 225–235.
- 13 M. Lei, C. Guo, L. Hua, S. Xue, D. Yu, C. Zhang and D. Wang, *Inflammation*, 2017, **40**, 2086–2093.
- 14 H. N. Englyst, S. M. Kingman and J. Cummings, *Eur. J. Clin. Nutr.*, 1992, **46**, S33–S50.
- 15 C. Ramirez, C. Millon, H. Nunez, M. Pinto, P. Valencia, C. Acevedo and R. Simpson, *Food Hydrocolloids*, 2015, **44**, 328–332.
- 16 I. Goñi, A. Garcia-Alonso and F. Saura-Calixto, *Nutr. Res.*, 1997, **17**, 427–437.
- 17 S. Ren, K. Li and Z. Liu, *J. Agric. Food Chem.*, 2019, **67**, 8617–8625.
- 18 H. Ali, P. Houghton and A. Soumyanath, *J. Ethnopharmacol.*, 2006, **107**, 449–455.
- 19 X. Peng, G. Zhang, Y. Liao and D. Gong, *Food Chem.*, 2016, **190**, 207–215.
- 20 H. Wu, W. Zeng, L. Chen, B. Yu, Y. Guo, G. Chen and Z. Liang, *Int. J. Biol. Macromol.*, 2018, **114**, 1194–1202.
- 21 H. Shumoy and K. Raes, *Food Chem.*, 2017, **229**, 381–387.
- 22 K. Liu, C. Chi, X. Huang, X. Li and L. Chen, *Food Chem.*, 2019, **278**, 560–567.
- 23 M. Wang, Q. Shen, L. Hu, Y. Hu, X. Ye, D. Liu and J. Chen, *Food Hydrocolloids*, 2018, **81**, 191–199.
- 24 F. van de Velde, J. van Riel and R. H. Tromp, *J. Sci. Food Agric.*, 2002, **82**, 1528–1536.
- 25 J. L. Jane, T. Kasemsuwan, S. Leas, H. Zobel and J. F. Robyt, *Starch - Stärke*, 1994, **46**, 121–129.
- 26 L. Chen, Q. Tong, F. Ren and G. Zhu, *Int. J. Biol. Macromol.*, 2014, **66**, 325–331.
- 27 S.-H. Jo, C.-Y. Cho, J.-Y. Lee, K.-S. Ha, Y.-I. Kwon and E. Apostolidis, *BMC Complementary Altern. Med.*, 2016, **16**, 1–7.
- 28 H. Kurihara, H. Fukami, S. Asami, Y. Toyoda, M. Nakai, H. Shibata and X.-S. Yao, *Biol. Pharm. Bull.*, 2004, **27**, 1093–1098.
- 29 L. Sun, F. J. Warren, G. Netzel and M. J. Gidley, *J. Funct. Foods*, 2016, **26**, 144–156.
- 30 L. M. Yue, J. Lee, L. Zheng, Y. D. Park, Z. M. Ye and J. M. Yang, *Int. J. Biol. Macromol.*, 2017, **103**, 829–838.
- 31 Z. Yang, C. Qin, P. Weng, X. Zhang, Q. Xia, Z. Wu, L. Liu and J. Xiao, *Int. J. Food Sci. Technol.*, 2020, **55**, 2531–2540.
- 32 R. Ferrer-Gallego, R. Gonçalves, J. C. Rivas-Gonzalo, M. T. Escribano-Bailón and V. de Freitas, *Food Chem.*, 2012, **135**, 651–658.
- 33 M. A. Castanho and M. J. Prieto, *Biochim. Biophys. Acta, Biomembr.*, 1998, **1373**, 1–16.
- 34 L. Sun, F. J. Warren and M. J. Gidley, *Food Hydrocolloids*, 2018, **79**, 63–70.
- 35 M. Wang, J. Jiang, J. Tian, S. Chen, X. Ye, Y. Hu and J. Chen, *J. Funct. Foods*, 2019, **56**, 286–294.
- 36 P. Alam, S. K. Chaturvedi, T. Anwar, M. K. Siddiqi, M. R. Ajmal, G. Badr, M. H. Mahmoud and R. H. Khan, *J. Lumin.*, 2015, **164**, 123–130.
- 37 Y. Q. Li, F. C. Zhou, F. Gao, J. S. Bian and F. Shan, *J. Sci. Food Agric.*, 2009, **57**, 11463–11468.
- 38 H. Ding, X. Hu, X. Xu, G. Zhang and D. Gong, *Int. J. Biol. Macromol.*, 2018, **107**, 1844–1855.

